RGNZ/MGPB

Trace element distribution in soils of the Bohdanka coal mine impact zone (Lublin coal basin): a geochemical perspective

Rudarsko-geološko-naftni zbornik
(The Mining-Geology-Petroleum Engineering Bulletin)
DOI: 10.17794/rgn.2026.5.5

Original scientific paper

CC BY

Vasyl Popovych[1], Viktor Skrobala[2], Victoria Serhiyenko[3], Taras Boyko[1], Yevhen Kobko[4], Nazarii Koval[1], Oksana Telak[5], Ostap Kit[1], Iryna Fediv[1]*

[1] *Lviv State University of Life Safety, Kleparivska Str. 35, Lviv, 79007, Ukraine.*

[2] *Department of Landscape Architecture, Horticulture and Urban Ecology, Ukrainian National Forestry University, 103 Gen. Chuprynky Str., Lviv, 79057, Ukraine.*

[3] *Danylo Halytsky Lviv National Medical University, 69 Pekarska Str., Lviv, 79010, Ukraine.*

[4] *Department of administrative and legal disciplines of the educational and scientific institute of law and psychology, National academy of internal affairs, Solomyanska Square, 1, Kyiv, 03035, Ukraine.*

[5] *Fire Service Academy, Słowackiego 52/54, 01-629 Warszawa, Poland.*

Abstract

This study presents the results of investigations of chemical element content in soils within the influence zone of a coal mine waste dump and focuses on the Bohdanka coal mine (Lublin Coal Basin) and its impact on surrounding ecosystems. The geochemical information is based on data on the concentration of 12 chemical elements (P, S, Ti, Y, Zr, Cu, Zn, Pb, Ni, V, Mn, Sr) in soils at six sites affected by the waste dump. Mathematical modelling was carried out by establishing relationships between chemical element concentrations. Based on the absolute content in the soils of the studied areas, the following groups of microelements were identified: I – Ti (4854 mg/kg); II – S (804 mg/kg); III.1 – P, Mn, Zr (353–590 mg/kg); III.2 – V, Sr, Zn (86–145 mg/kg); III.3 – Pb, Y, Ni, Cu (21–26 mg/kg). Site No. 4 (foot of the rock dump) is characterised by a hazardous level of soil pollution (total pollution index Zc = 53.1–76.5), while site No. 2 is at the upper limit of the permissible level of pollution with a transition to a moderately hazardous zone (Zc = 10.8–15.1). Other sites are characterised by permissible levels of pollution. Discriminant analysis enabled the determination of the distribution of microelements in the upper soil layers by depth, forming a geochemical sequence of 5 cm → 10 cm → 15 cm. The developed mathematical models make it possible to refine ecological gradients of chemical element distribution in soils, primarily heavy metals, in the upper soil layers.

Keywords:
coal mine; rock dump; trace elements; geochemical processes; environmental safety; technological safety; human health

1. Introduction

Nowadays, with the bleak environmental situation, the issues of man-made pollution of soil, water bodies and air as a result of mining operations are particularly acute (**Pukish et al., 2024; Bun et al., 2024**). One of the negative factors contributing to environmental pollution in coal mining regions is coal mine waste dumps, which are a powerful source of long-term secondary pollution of ecosystems and cause diseases in people living in these regions (**Serhiyenko & Serhiyenko, 2019**). Extensive research has been conducted on coal-mining regions in various aspects. Researchers have concluded that the most dangerous factor affecting environmental safety and human health is the entry of chemical compounds and substances, as well as individual elements, into the body (**Nersesyan et al., 2021; Serhiyenko et al., 2024**). In particular, the highest concentrations of NH_4^+, HCO_3^-, F^-, Cl^-, Br^-, NO_2^-, NO_3^-, PO_4^{3-}, SO_4^{2-}, Al, B, Ba, Ca, Cd, Cr, Cu, Fe, K, Li, Mg, Mn, Na, P, Pb, S, Si, Sr, Zn are observed in areas of high thermal activity, as inorganic components are converted into more water-soluble forms. Since the thermal activity of the dump shows a regional pattern, it also follows that the concentrations of elements and ions in the discharge waters demonstrate significant regional differences (**Lewińska-Preis et al., 2021; Adamenko et al., 2017**).

Samples collected from the Upper Silesian coal basin dumps were used to assess the content of organic and inorganic pollutants, including polycyclic aromatic hydrocarbons and trace elements (Pb, Cd, Cr, Cu, Zn, Ni, Hg, As). Previous studies have shown that elevated concentrations of mercury and lead are associated with their migration from deeper parts of the dumps due to thermal processes. High levels of Hg, Pb, and Cd, as well as the

* Corresponding author: Iryna Fediv
e-mail address: ira.arnaut94@gmail.com
Received: 19 February 2026. Accepted: 05 May 2026.
Available online: 26 October 2026

presence of chlorinated surfactants and nitrogen heterocycles formed or enriched during self-heating, indicate a significant environmental hazard (**Nádudvari et al., 2021**). A combustion zone of the spoil tip was investigated, where increased soil temperatures were recorded. Soil analyses were carried out for different grain-size fractions, which made it possible to assess the variability of the chemical composition depending on particle size. The results indicate that heavy metals such as Mn, Zn, Pb, and Cu are predominant among trace elements, while Fe and Ca dominate among major elements. In addition, elevated contents of organic carbon were identified in combination with polycyclic aromatic hydrocarbons, confirming the complex nature of contamination in such environments (**Abramowicz et al., 2021**).

Despite the large number of waste dumps identified in Polish coal basins, their environmental impact has been studied unevenly. For example, although 116 waste dumps are located in the Lower Silesian Coal Basin, where mining activities ceased in 2000, their relatively small surface area and thermal condition have limited detailed analysis (**Marcisz et al., 2020**).

In addition to the input of hazardous substances and compounds into biota from coal mine waste dumps as a result of geochemical processes, a significant amount of substances is released into the environment as a consequence of waste rock combustion (**Popovych & Voloshchyshyn, 2019; Pukish et al., 2023; Tatsiy et al., 2019**). In soil samples affected by thermal impacts of fires, an increase in mercury content in the mobile fraction was observed, indicating that the combustion of mining residues increases the mobility, toxicity, and bioavailability of mercury, thereby enhancing the pollution potential of coal waste dumps (**Monteiro et al., 2024**). More than 50 years after the cessation of mining activities, the spoil tip of a former uranium and coal mine is still a source of pollution of water and river sediments. While the burned part constitutes the main source of sulfate, lead, and other volatile elements (Cd, Se) accumulated during combustion processes, the unburned part is a source of uranium and molybdenum (**Bohdan et al., 2018**).

A number of studies are devoted to the physiological resistance and phytoremediation properties of plants and microorganisms in the impact zone of waste dumps (**Popovych et al., 2021**). Specifically, aimed to minimize the mobility of heavy metals (As, Cu, Cd, Ni, Pb, and Se), improve soil health, and stimulate plant growth (phytoremediation using Lolium perenne L.) (**Salgado et al., 2024**). It was found that the combination of dunite and compost successfully reduced the concentration of available Cu and Ni in soil by more than four times, significantly improved soil properties, and promoted higher biomass production. In addition, Lolium perenne L. demonstrated phytostabilization capacity for Cu and Ni in soils treated with soil amendments.

An analysis of heavy metal content shows that they are higher in plant materials (Calamagrostis epigejos, Solidago canadensis) than in soil materials within the plant root zone. Statistical analysis indicates a positive correlation between the content of trace elements in plants (roots and aboveground parts) and soil samples in both thermally active and inactive zones (**Abramowicz & Rahmonov, 2024**).

Arabidopsis halleri and Arabidopsis arenosa accumulate large amounts of Zn in their tissues, particularly in stem leaves. Among 22 identified bacterial taxa, the highest level of taxonomic diversity ($H' = 2.01$) was detected in the leaves of A. halleri. A total of 96%, 98%, 99%, and 98% of the studied strains exhibited resistance to Cd, Zn, Pb, and Cu, respectively. Nine bacterial strains isolated from waste dumps were resistant to toxic metals and are considered potential bioremediation agents (**Oleńska et al., 2023**).

The most effective methods for reducing the negative impacts of waste dumps are reclamation and phytomelioration. Due to the natural transformative function of vegetation cover, the level of ecotope pollution and its impact on human health are reduced (**Skrobala et al., 2020**). It should be noted that sustainable reclamation methods were investigated at the largest coal mine in the United States, located in Wyoming. These methods included post-mining landform reconstruction to the original contour and the restoration of a stable hydrological system for surface water drainage (**Krzyszowska Waitkus, 2022**). Studies of the chemical element content in soils within the impact zones of waste dumps represent a relevant issue of contemporary international research, as the geochemical migration of hazardous substances and compounds directly affects biota and human health (**Serhiyenko & Serhiyenko, 2022**).

Despite numerous studies on soil contamination in mining areas, the spatial distribution of trace elements within the impact zones of coal mine waste dumps remains insufficiently investigated. In particular, there is a lack of detailed geochemical studies for specific sites such as the “Bohdanka” coal mine waste dump. The present study is aimed at assessing the spatial distribution of trace elements in soils within the impact zone of the waste dump and identifying the main patterns of their geochemical differentiation using statistical and mathematical approaches.

2. Methods

The object of this study is the “Bohdanka” coal mine (Lublin Coal Basin). Only one waste dump is located in the Lublin Coal Basin (see **Figure 1**). In the Lublin Basin, coal-bearing seams are represented by Upper Carboniferous deposits, mainly of late Bashkirian age, formed in paralic sedimentary environments (**Nieć et al., 2023**). The average total sulfur content in the basin seams reaches 1.27% in seam 382 and 0.99% in seam 385/2. The total sulfur content varies within the range of

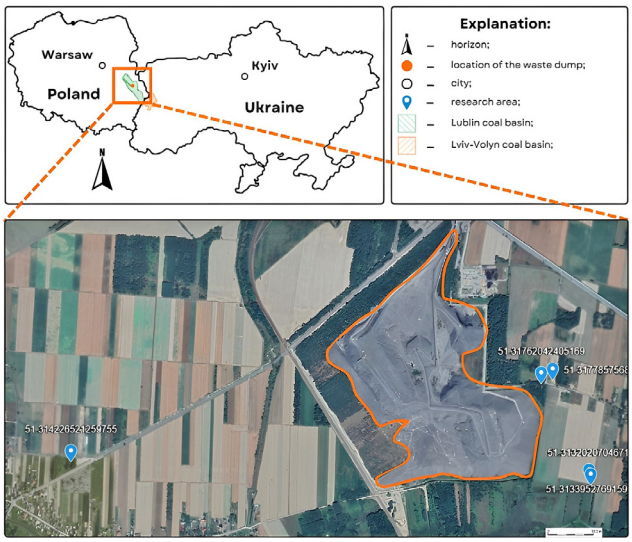


Figure 1: Location scheme of the "Bohdanka" coal mine within the coal basin (coordinates: 51.31882, 23.00494)

0.82–2.16% in seam 382 and 0.58–1.83% in seam 385/2 (**Misiak, 2012**).

The Lublin Coal Basin is located in eastern Poland and represents a Carboniferous coal-bearing formation developed within the Lublin Trough. The basin is composed predominantly of mudstones, claystones, sandstones, and coal seams formed under paralic depositional conditions (**Krzeszowska, 2019; Nieć et al., 2023**). Coal-bearing strata belong mainly to the Upper Carboniferous (Pennsylvanian), particularly the late Bashkirian stage (**Nieć et al., 2023**). The coal seams exploited by the "Bohdanka" mine (notably seams 382 and 385/2) are characterized by relatively stable thickness, low to moderate sulfur content, and a relatively simple geological structure compared to other European coal basins (**Misiak, 2012**). The overburden consists mainly of fine-grained clastic rocks, which influence the geochemical background of soils formed in the mine impact zone. The geological structure and lithological composition of the coal-bearing sequence play a key role in the formation of trace element distribution patterns in soils, as they determine both the primary geochemical background and the mobility of elements under anthropogenic impact conditions. Mining and geological conditions of coal deposits significantly influence the formation of technogenic landscapes and the redistribution of trace elements in soils within mining areas (**Lyashenko et al., 2022; Krzeszowska, 2019**).

Soil sampling was carried out within the impact zone of the waste dump at six representative sites located at different distances from the dump, including the foot of the waste dump, areas of natural soil, forested areas, and zones influenced by drainage processes (see **Figure 1**). The selection of sampling sites was based on differences in land use, vegetation cover, and the expected degree of technogenic impact. At each site, soil samples were collected at three depths: 5 cm, 10 cm, and 15 cm, corresponding to the upper soil horizons most affected by anthropogenic influence. Sampling was performed during the spring period under stable weather conditions. At each depth, composite samples were formed by mixing several subsamples collected within a radius of 1–2 m to ensure representativeness. The determination of chemical element concentrations in soil samples was carried out using X-ray fluorescence analysis (XRF) in accordance with standard analytical procedures.

The assessment of the soil contamination level within the impact zone of the waste dump was carried out using indicators developed on the basis of geochemical and hygienic environmental studies. These indicators include the concentration coefficient Kc, the total pollution index Zc, and the soil pollution index (**Shmatkov & Yakovishina, 2018**).

The concentration coefficient Kc is expressed by **Equations 1** and **2**:

$$Kc_i = \frac{C_i}{C_{MPK_i}}, \text{ times} \quad (1)$$

$$Kc_i = \frac{C_i}{C_{BV_i}}, \text{ times} \quad (2)$$

Where:

C - is the actual concentration of the chemical element iii in the soil (mg/kg);

C_{MPK} - is the maximum permissible concentration of the chemical element i (mg/kg);

C_{BV} - is the background concentration of the chemical element i (mg/kg);

i - is the ordinal number of the chemical element.

Background concentrations of chemical elements were determined based on the analysis of literature sources (**Fatieiev & Pashchenko, 2003**).

The soil pollution index PI (pollution index) is expressed by **Equation 3**:

$$PI = \sum_{1}^{n} Kc_i/n, \text{ times} \quad (3)$$

Where:

n - is the number of chemical elements.

The total pollution index Zc is expressed by **Equation 4**:

$$Zc = \sum_{1}^{m} Kc_i\text{-}(m\text{-}1), \text{ times} \quad (4)$$

Where:

m - is the number of concentration coefficients exceeding 1.

For the total pollution index Zc, the following pollution categories have been established empirically:

– permissible – Zc<16;
– moderately hazardous – Zc=16...32;
– hazardous – Zc=32...128;
– extremely hazardous – Zc>128.

The features of the spatial distribution of chemical elements within the waste dump impact zone were studied using data mining methods (**Kantardzic, 2020**). The study included three main stages: investigation of the structure of mutual spatial arrangement of elementary sites in the multidimensional feature space of chemical element concentrations, mathematical modelling of the structure, and verification of the mathematical model (**Popovych et al., 2025**).

The basis of the geochemical information consisted of data on the concentrations of 12 chemical elements (P, S, Ti, Y, Zr, Cu, Zn, Pb, Ni, V, Mn, Sr) in soils at six sites within the waste dump impact zone. Mathematical modelling was performed by identifying systematic relationships between chemical element concentrations. Each site can be represented as a point in a multidimensional feature space, the coordinates of which correspond to the concentration values of chemical elements. In this case, the similarity of sites based on the set of environmental pollution parameters can be determined using distances between points. The essence of the subsequent mathematical procedure consists in identifying the axes of maximum variation, determining their number, and assessing the contribution of each chemical element to the variation based on principal component analysis.

The assessment of differences between ecotope parameters within the waste dump impact zone was performed using analysis of variance. The construction of a typological scheme of mine ecotopes and graphical visualization of the results of mathematical modelling were carried out based on canonical discriminant analysis (**Skrobala, 2022a**). Verification of the mathematical model was performed based on a comparative assessment of site positions along the axes of maximum variation (multidimensional ordination) with the results of studies of soil and vegetation cover (**Skrobala, 2022b**).

Standardized values of chemical element concentrations were calculated using the **Equations 5**:

$$z_i = (x_i\text{-}M)/\sigma, \quad (5)$$

Where:

- Z_i - the standardized value of the chemical element concentration in soil;
- x_i - the actual concentration of the chemical element i;
- M - the arithmetic mean concentration of the chemical element in soil;
- σ - the standard deviation of the chemical element concentration in soil.

3. Results and Discussion

The content of chemical elements in soil depends on many factors, primarily on their content in the parent material. The highest concentrations in soils are usually characteristic of macroelements, including Si, Al, Fe, Ca, Mg, K, Na, and C. These elements are almost entirely inherited from the soil-forming material and are redistributed within the soil profile during the process of soil formation. A transitional group between macro- and microelements is formed by Ti, Mn, N, P, and S; their content in soils varies from hundredths to tenths of a percent (see **Tables 1–2**). The content of typical trace elements is less than $n\times10^{-3}$ %, and this group includes Cu, Co, Ni, V, Sr, Li, Mo, and other elements (**Kyrylchuk & Bonishko, 2011**).

Grouping elements according to their concentration in soil is the simplest operation and is primarily used to identify the role of individual elements in soil mass formation. The concentration levels of chemical elements in ecotopes within the impact zone of the studied waste dump are presented in **Table 1**.

Based on the absolute content in the soils of the studied sites (see **Table 1**), the following groups of trace elements can be distinguished:

I – Ti (mean concentration value of 4854 mg/kg);

II – S (mean concentration value of 804 mg/kg);

III.1 – P, Mn, Zr (mean concentration values of 353–590 mg/kg);

III.2 – V, Sr, Zn (mean concentration values of 86–145 mg/kg);

III.3 – Pb, Y, Ni, Cu (mean concentration values of 21–26 mg/kg).

Spatial mapping and surface modelling of chemical element concentrations (see **Figures 2** and **3**) were performed using interpolated data based on a regular grid. A local Cartesian coordinate system was applied, where X corresponds to Easting (0–24 m) and Y to Northing (−4–10 m). The spatial distribution of concentrations was visualized using filled contour maps with labeled isolines, constructed with a regular contour interval of 200 mg/kg. Surface modelling was carried out using an interpolated grid generated by the inverse distance weighting (IDW) method (power = 2). Three-dimensional visualization included both wireframe surfaces and combined color surfaces with contour lines and sampling points. Cross-sectional profiles were additionally constructed along the Easting direction at a fixed Northing value (Y = 5 m) to illustrate changes in concentration. Sampling points are indicated on the maps and labeled with measured concentration values.

The spatial distribution of Ti within the studied sites in the 0–5 cm soil horizon is presented in **Figure 2**.

The spatial distribution of S within the studied sites in the 0–5 cm soil horizon is graphically presented in **Figure 3**.

Compared to the mean values, site No. 4 reveals elevated concentrations of 9 out of 12 chemical elements: S, Ti, V, Ni, Cu, Zn, Sr, Y, and Pb (see **Tables 1–2**). Only P exhibits a low concentration at this site. Statistical parameters of chemical element content in the soils of the studied sites, used for further calculations of z_i, are presented in **Table 2**.

Table 1: The concentration levels of chemical elements in ecotopes within the impact zone

No	h	Concentration of the chemical elements, mg/kg											
		Ti	S	P	Mn	Zr	V	Sr	Zn	Pb	Y	Ni	Cu
1	5	3663.2	141.9	598.2	203.9	376.0	125.8	50.1	25.4	11.7	15.2	12.3	8.2
	10	3061.0	159.9	577.1	213.4	254.6	126.8	50.5	7.5	15.7	2.2	11.5	11.6
	15	2572.7	123.0	593.5	207.7	238.8	126.0	46.0	30.0	12.0	13.8	15.6	7.9
2	5	4231.2	974.6	617.6	487.7	335.7	73.8	80.6	36.1	22.4	22.5	19.2	23.1
	10	5881.9	1940.7	634.5	402.5	335.4	60.1	112.9	34.4	37.0	27.7	20.8	26.0
	15	4610.5	1372.8	610.2	323.3	325.4	130.2	89.2	6.8	35.9	25.2	11.7	23.4
3	5	5202.1	114.5	603.1	491.2	606.6	153.5	97.9	34.9	20.2	35.4	12.1	10.5
	10	5006.6	66.9	588.1	405.8	505.2	147.5	88.7	23.5	17.8	28.7	12.6	12.6
	15	4060.4	39.8	553.5	417.5	378.2	127.0	65.3	18.6	14.0	21.4	12.0	7.5
4	5	8095.4	2867.0	524.0	318.1	219.0	199.5	284.5	170.1	53.0	56.9	72.0	66.9
	10	7986.7	2229.3	524.4	375.8	220.7	247.0	273.7	340.2	49.7	56.7	80.5	63.8
	15	7910.8	1993.6	511.7	379.1	219.5	209.2	267.8	690.6	50.0	52.9	74.5	58.7
5	5	4782.1	135.6	608.2	547.2	513.3	144.7	70.8	35.7	21.0	25.8	12.3	9.4
	10	4101.1	46.6	571.2	498.7	491.1	127.3	67.7	31.0	18.1	26.2	11.0	7.5
	15	4264.2	43.1	577.8	450.4	498.6	126.7	67.1	24.8	19.1	27.0	11.5	8.5
6	5	3969.2	951.0	652.1	296.6	185.5	160.9	36.0	26.6	21.0	2.4	14.2	10.3
	10	4665.7	766.1	639.8	260.8	403.7	164.4	46.2	8.7	21.4	16.4	16.0	9.8
	15	3302.3	507.5	632.3	377.0	249.3	152.9	44.7	8.1	24.5	2.5	13.4	9.0
BV	-	4600*	1200*	1200*	1500	255.6*	150	458*	23	32	23.4*	4	3
		Concentration coefficient *Kc*, exceeding background values or MPCs, times											
1	5	0.80	0.12	0.50	0.14	1.47	0.84	0.11	1.10	0.37	0.65	3.07	2.72
	10	0.67	0.13	0.48	0.14	1.00	0.85	0.11	0.33	0.49	0.09	2.88	3.86
	15	0.56	0.10	0.49	0.14	0.93	0.84	0.10	1.30	0.38	0.59	3.90	2.64
2	5	0.92	0.81	0.51	0.33	1.31	0.49	0.18	1.57	0.70	0.96	4.81	7.68
	10	1.28	1.62	0.53	0.27	1.31	0.40	0.25	1.50	1.16	1.18	5.20	8.67
	15	1.00	1.14	0.51	0.22	1.27	0.87	0.19	0.29	1.12	1.08	2.93	7.79
3	5	1.13	0.10	0.50	0.33	2.37	1.02	0.21	1.52	0.63	1.51	3.01	3.52
	10	1.09	0.06	0.49	0.27	1.98	0.98	0.19	1.02	0.55	1.23	3.16	4.19
	15	0.88	0.03	0.46	0.28	1.48	0.85	0.14	0.81	0.44	0.91	3.01	2.49
4	5	1.76	2.39	0.44	0.21	0.86	1.33	0.62	7.40	1.66	2.43	17.99	22.31
	10	1.74	1.86	0.44	0.25	0.86	1.65	0.60	14.79	1.55	2.42	20.13	21.27
	15	1.72	1.66	0.43	0.25	0.86	1.39	0.58	30.03	1.56	2.26	18.63	19.57
5	5	1.04	0.11	0.51	0.36	2.01	0.96	0.15	1.55	0.66	1.10	3.09	3.13
	10	0.89	0.04	0.48	0.33	1.92	0.85	0.15	1.35	0.56	1.12	2.75	2.49
	15	0.93	0.04	0.48	0.30	1.95	0.84	0.15	1.08	0.60	1.15	2.87	2.84
6	5	0.86	0.79	0.54	0.20	0.73	1.07	0.08	1.16	0.66	0.10	3.54	3.44
	10	1.01	0.64	0.53	0.17	1.58	1.10	0.10	0.38	0.67	0.70	4.00	3.25
	15	0.72	0.42	0.53	0.25	0.98	1.02	0.10	0.35	0.77	0.11	3.35	3.01

Legend: No. – site number; 1 – natural soil; 2 – *Robinia pseudoacacia* plantation; 3 – lake shoreline; 4 – foot of the waste dump, drainage sludge; 5 – birch forest; 6 – pine forest. h – soil sampling depth, cm; M – mean value, mg/kg; σ – standard deviation, mg/kg; BV – background concentration value (*) or maximum permissible concentration (MPC), mg/kg.

At site No. 2, elevated concentrations are characteristic of P, S, Mn, and Pb. Maximum concentrations of Mn and Zr are observed at sites No. 3 and No. 5, while the maximum concentration of P is characteristic of site No. 6. In general, based on the absolute content of chemical elements in soil, three groups of sites can be distinguished:

1 – site No. 4;
2 – site No. 2;
3 – sites No. 3, 5, 1, and 6.

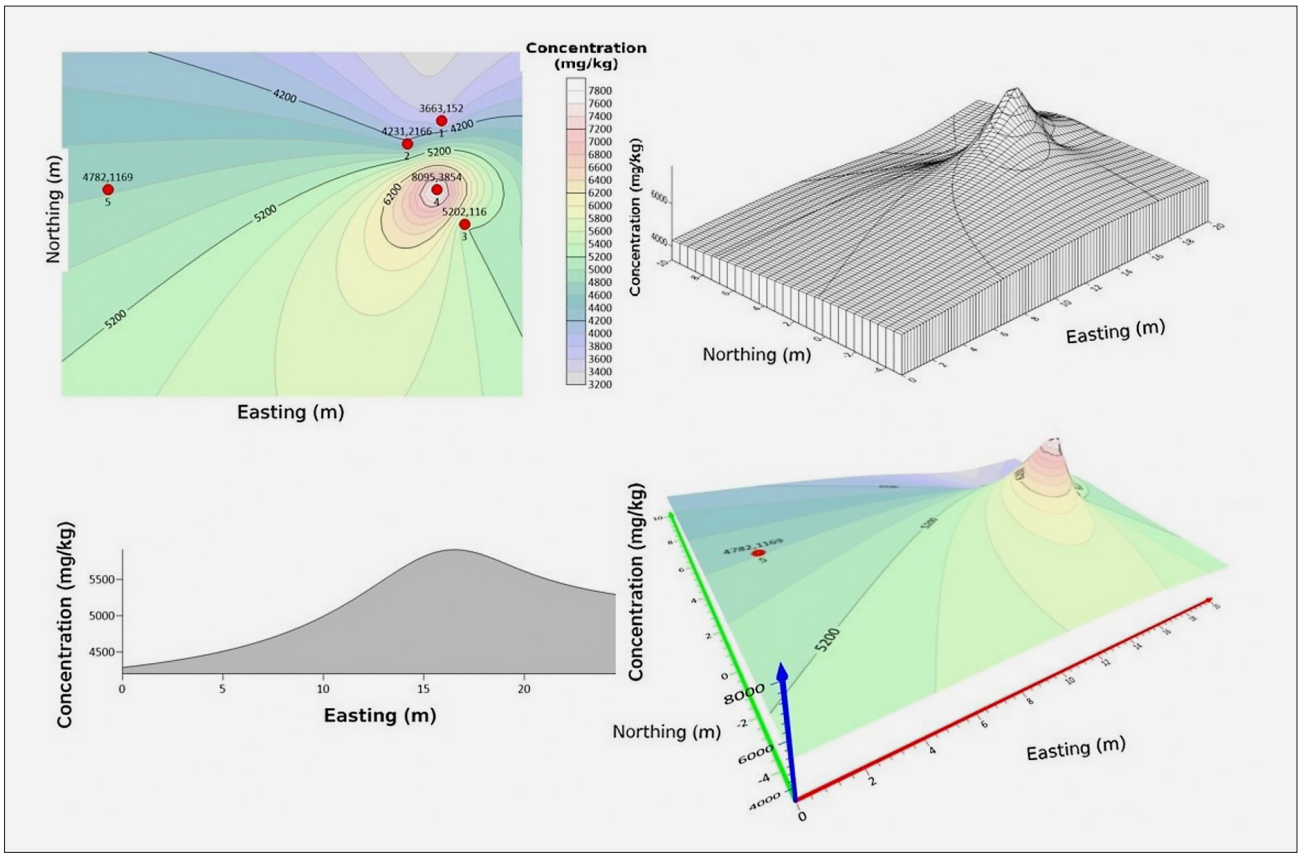


Figure 2: Distribution of Ti within the studied sites in the 0–5 cm soil horizon

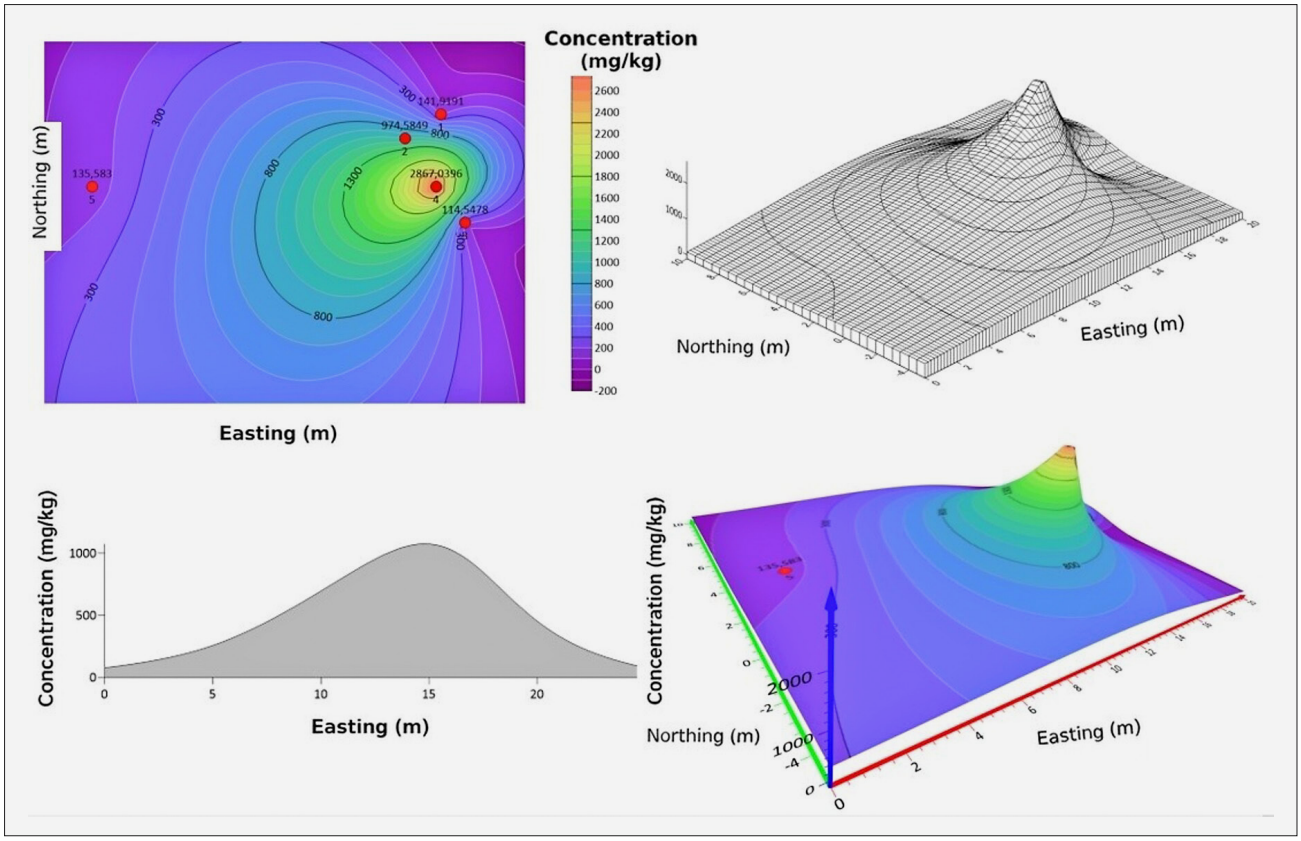


Figure 3: Distribution of S within the studied sites in the 0–5 cm soil horizon

Table 2: Descriptive Statistics of trace element content in soil

Chemical element	Descriptive Statistics					
	Mean	Minimum	Maximum	Standard Deviation	Standard Error	Concentration Coefficient (Kc)
	Concentration of chemical elements, mg/kg					
Ti	4853.7	2572.7		1643.63	387.4	1.1
S	804.1	39.8	2867.0	906.76	213.7	0.7
P	589.9	511.7	652.1	41.05	9.7	0.5
Mn	369.8	203.9	547.2	105.26	24.8	0.2
Zr	353.1	185.5	606.6	126.81	29.9	1.4
V	144.6	60.1	247.0	43.92	10.4	1.0
Sr	102.2	36.0	284.5	82.30	19.4	0.2
Zn	86.3	6.8	690.6	171.09	40.3	3.8
Pb	25.8	11.7	53.0	13.36	3.1	0.8
Y	25.5	2.2	56.9	16.77	4.0	1.1
Ni	24.1	11.0	80.5	23.94	5.6	6.0
Cu	20.8	7.5	66.9	20.35	4.8	6.9

The content of individual chemical elements in soil may be low; however, their concentrations may significantly exceed background values or maximum permissible concentrations (MPC). This primarily applies to heavy metals. In this regard, an important characteristic of chemical elements is the value of concentration coefficients, which indicate exceedances of maximum permissible concentrations for heavy metals and background values for other trace elements. The maximum exceedance of MPC at the studied sites is characteristic of three chemical elements (see **Table 2**): Cu (MPC exceedance within the range of 2.5–22.3 times), Ni (MPC exceedance within the range of 2.8–20.1 times), and Zn (MPC exceedance within the range of 0.3–30.0 times). The highest values of the soil pollution index (PI = 7.36–10.29 times) are characteristic of site No. 4, followed by site No. 2 (PI = 1.92–2.49 times). For the remaining sites, the soil pollution index does not exceed 1.5 times.

Site No. 4 is characterized by a hazardous level of soil contamination (Zc = 53.1–76.5), while site No. 2 is located at the upper limit of the permissible contamination level with a transition to the moderately hazardous category (Zc = 10.8–15.1). The remaining sites are characterized by a permissible level of contamination (see **Table 2**).

Based on the values of concentration coefficients (see **Tables 1–2**), the following groups of chemical elements can be distinguished (see **Figure 4a**):

1. Cu, Ni, Zn (mean concentration coefficient values of 3.8–6.9 times);
2. Zr, Y, Ti, V, Pb, S (mean concentration coefficient values of 0.7–1.4 times);
3. P, Mn, Sr (mean concentration coefficient values of 0.2–0.5 times).

Such differentiation of chemical elements reflects general patterns of trace element distribution in technogenically disturbed soils. The observed distribution patterns of trace elements are consistent with previous studies conducted in coal mining regions. For example, soils from the Upper Silesian coal basin dumps were reported to contain high concentrations of trace elements such as Mn, Zn, Pb, and Cu, as well as elevated levels of major elements including Fe and Ca (**Abramowicz et al., 2021**). In addition, significant enrichment in mercury and lead has been associated with thermal processes within spoil heaps (**Nádudvari et al., 2021**), which supports the patterns observed in the present study. These findings confirm that the formation of geochemical anomalies in soils is controlled by both anthropogenic inputs and processes of element migration within the soil profile.

From an environmental perspective, the identified patterns of trace element distribution can be explained by several key mechanisms of element migration within the waste dump impact zone. First, the elevated concentrations of Cu, Zn, and Ni at site No. 4 indicate their accumulation due to surface runoff and leaching processes from the waste dump body. These elements are known to be mobile under conditions of increased moisture and can be transported with drainage waters. Second, thermal processes within the waste dump contribute to the transformation of mineral phases and increase the mobility of certain elements, particularly heavy metals. This leads to their secondary redistribution in adjacent soils. Third, the role of vegetation and soil properties is also significant, as plant cover can influence both the accumulation and stabilization of trace elements through biogeochemical processes. Thus, the spatial differentiation of chemical elements in soils reflects a combination of primary geogenic background, technogenic input from the waste dump, and subsequent migration processes controlled by hydrological and physicochemical conditions.

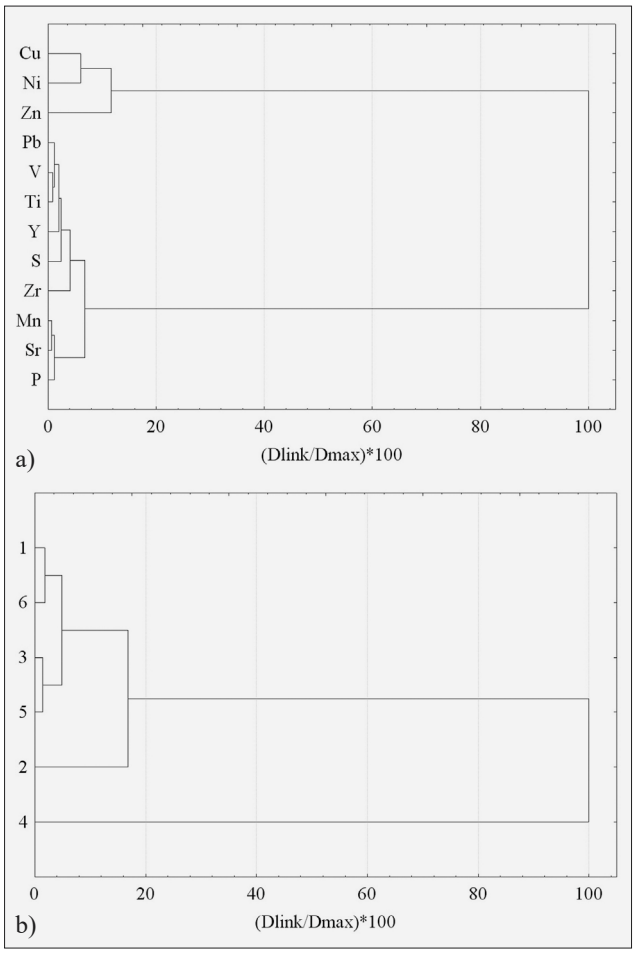


Figure 4: Dendrogram of similarity of trace elements (a) and sites (b) based on concentration coefficients (legend: numerical site numbering is given in **Table 1**)

The maximum Euclidean distance is observed between Cu and Mn (DE = 23.0), Cu and Sr (DE = 22.7), and Cu and P (DE = 22.6). The differentiation of chemical elements based on Euclidean distances in two-dimensional space can be represented as a triangle, at the vertices of which are located: (1) Ni; (2) Cu; (3) Mn and the remaining chemical elements, with Zn positioned in the center. In three-dimensional space, Cu is located at the top of a three-dimensional pyramid, the base of which is a triangle formed by Zn, Ni, and Mn together with the remaining trace elements.

Based on the values of concentration coefficients (see **Tables 1–2**), three groups of sites can similarly be distinguished (see **Figure 4b**):

1 – site No. 4;

2 – site No. 2;

3 – sites No. 1, 6, 3, and 5.

The differentiation of sites based on Euclidean distances in two-dimensional space can be represented as a triangle, at the vertices of which are located sites 4, 2, and 5+3. The largest Euclidean distance relative to other ecotopes is characteristic of site No. 4 (DE = 25.5–29.5), whereas for the remaining sites it averages DE = 7.5–9.3.

Analysis of the relationships between chemical element concentrations in soil indicates the presence of strong associations between them (see **Table 3**). Correlation coefficients show high values for many pairs of chemical elements. In particular, for Cu and Sr concentrations r = 0.98, for Cu and Ni r = −0.97, for S and Pb r = 0.95, for Ti and Sr r = 0.95, and for Ni and Sr r = 0.97. Only Mn and, partially, Zr exhibit weak relationships with other chemical elements.

The conceptual framework of the study is based on mathematical modelling of the spatial structure of the studied sites in a multidimensional space, the features of which are represented by chemical element contents in soil. Since the concentrations of chemical elements in the soils of the studied sites are correlated with each other, it can be concluded that the observational data can be explained by a small number of new variables that are not measured directly but can be obtained through linear combinations of the original data. This makes it possible to reduce the dimensionality of the observation space. Graphically, the calculation procedure is reduced to shifting the origin of coordinates to the data center and rotating the coordinate axes in such a way that the abscissa is oriented in the direction of maximum variance of the data set.

The results of principal component analysis based on the correlation matrix are as follows (see **Figure 5**):

$$\begin{aligned}\text{Factor}_1 = {} & 0.259\times P - 0.300\times S - 0.330\times Ti - \\ & - 0.307\times Y + 0.154\times Zr - 0.345\times Cu - \\ & - 0.296\times Zn - 0.327\times Pb - 0.345\times Ni - \\ & - 0.250\times V - 0.009\times Mn - 0.348\times Sr,\ l_1 = 8.10 \end{aligned} \quad (5)$$

$$\begin{aligned}\text{Factor}_2 = {} & -0.136\times P - 0.179\times S + 0.167\times Ti + \\ & + 0.313\times Y + 0.617\times Zr - 0.058\times Cu - \\ & - 0.004\times Zn - 0.034\times Pb - 0.065\times Ni - \\ & - 0.052\times V + 0.654\times Mn + 0.064\times Sr,\ l_2 = 1.83 \end{aligned} \quad (6)$$

Where Factor_i are component coordinates representing complex environmental gradients; P, S, Ti, Y, Zr, Cu, Zn, Pb, Ni, V, Mn, and Sr are standardized values of chemical element concentrations in soil; and λ_i are the eigenvalues of the vectors.

Analysis of the eigenvalue characteristics l_i indicates that the two principal components account for 82.8% of the total variance; therefore, for many analytical purposes, it is sufficient to use a two-dimensional projection of the original data matrix (**Kantardzic, 2020**). The eigenvectors of the correlation matrix (5)-(6) make it possible to identify combinations of chemical element concentrations that define the axes of maximum variation of sites within the waste dump impact zone. The main pattern governing the formation of the geochemical state of the sites (the first principal component, Factor_1) is reflected in the following structure of relationships between chemical elements (see **Figure 5, Table 3**): as the con-

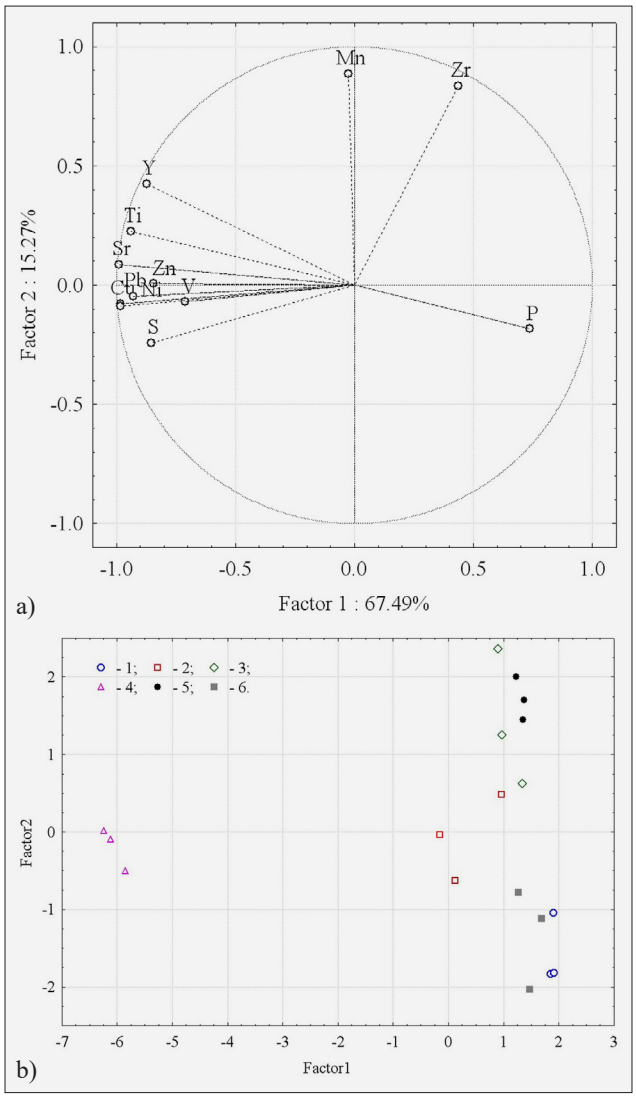


Figure 5: Results of principal component analysis of chemical element contents in soil: (a) system of relationships between chemical element concentrations and complex environmental gradients; (b) distribution of sites in the coordinate system of complex environmental gradients (legend: $Factor_{1-2}$ – principal components, complex environmental gradients; numerical site numbering is given in **Table 1**).

centrations of Sr (correlation coefficient r = −0.99), Ni (r = −0.98), Cu (r = −0.98), Ti (r = −0.94), Pb (r = −0.92), Y (r = −0.87), S (r = −0.85), Zn (r = −0.84), and V (r = −0.71) decrease in soil, the concentration of P increases (r = 0.74). The principal components (Factor1 and Factor2) represent complex environmental gradients formed by combined effects of trace element associations, reflecting both geogenic background and anthropogenic influence from the waste dump.

The first principal component explains 67.5% of the total variance; therefore, its values clearly reflect the main pattern of chemical element contents within the waste dump impact zone. Low values of the first principal component, $Factor_1$, are characteristic of site No. 4 (foot of the waste dump, drainage sludge) (see **Figure 4**), which is distinguished by high values of concentration coefficients, K_c, for 9 out of 12 chemical elements, particularly Cu, Zn, and Ni (see **Tables 1-2**). In contrast, the highest values of the first principal component are observed at sites No. 1 (natural soil) and No. 6 (pine forest), where low contents of the heavy metals Cu, Zn, and Ni were recorded (see **Tables 1-2**). The first axis of the ordination scheme reflects a decrease in the level of anthropogenic load, as evidenced by a strong negative correlation with the soil pollution index PI (pollution index) and the total pollution index Zc (in both cases, the correlation coefficient is r = -0.98).

The second axis of maximum variation, $Factor_2$, additionally explains 15.3% of the total data variance (see **Figure 4**). The value of the $Factor_2$ function mainly depends on the contents of Mn (r = 0.88) and Zr (r = 0.84). Minimum values of the $Factor_2$ function are characteristic of sites No. 1 (natural soil) and No. 6 (pine forest), which are distinguished by the lowest concentrations of Zr and Mn in soil (see **Table 1**). The highest values of the second principal component are observed at sites No. 5 (birch forest) and No. 3 (lake shoreline), for which an opposite trend in the contents of these chemical elements is characteristic. The third axis of maximum variation, $Factor_3$, which additionally explains 7.8% of the total data variance, mainly depends on the contents of S (r = -0.45) and P (r = -0.50). Minimum values of the $Factor_3$ function are characteristic of site No. 2 (*Robinia pseudoacacia* plantation).

Thus, in the two-dimensional space of complex environmental gradients, the ecotopes can be represented as a triangle, with site No. 2 (Robinia pseudoacacia plantation) located in the center and sites No. 4 (foot of the waste dump, drainage sludge), No. 1 (natural soil), and No. 5 (birch forest) at the vertices (see **Figure 4**). In three-dimensional space, site No. 2 occupies the apex of a triangular pyramid.

The dimensionality of the observation space can be reduced not only on the basis of principal component calculations of the correlation matrix but also by excluding from the analysis certain chemical elements whose presence is insignificant, taking into account their strong interrelationships (high correlation coefficients). The results of analysis of variance may also serve as a basis for further conclusions (see **Tables 4–5**).

One-factor analysis of variance is based on the calculation of the Fisher criterion, which represents the ratio of between-group variance to within-group variance. Between-group variance indicates the extent to which sites within the waste dump impact zone differ from each other in terms of chemical element concentration levels. Between-group variance equals zero when the mean concentrations of chemical elements are equal. Within-group variance characterizes differences in chemical element concentrations within the same site. The highest values of the Fisher criterion are characteristic of the chemical elements Cu, Ni, Sr, and Pb, which act as the main factors

Table 3: Matrix of relationships between trace element concentrations and PCA Factors

Chemical element	P	S	Ti	Y	Zr	Cu	Zn	Pb	Ni	V	Mn	Sr
P	1.00	-0.36	-0.62	-0.74	0.18	-0.68	-0.69	-0.51	-0.74	-0.58	-0.05	-0.77
S	-0.36	1.00	0.82	0.65	-0.59	0.91	0.59	0.95	0.83	0.42	-0.10	0.83
Ti	-0.62	0.82	1.00	0.92	-0.19	0.91	0.74	0.91	0.89	0.62	0.21	0.95
Y	-0.74	0.65	0.92	1.00	0.01	0.83	0.69	0.78	0.82	0.55	0.32	0.91
Zr	0.18	-0.59	-0.19	0.01	1.00	-0.51	-0.39	-0.46	-0.51	-0.30	0.60	-0.36
Cu	-0.68	0.91	0.91	0.83	-0.51	1.00	0.77	0.94	0.97	0.62	-0.02	0.98
Zn	-0.69	0.59	0.74	0.69	-0.39	0.77	1.00	0.71	0.84	0.64	0.03	0.81
Pb	-0.51	0.95	0.91	0.78	-0.46	0.94	0.71	1.00	0.88	0.56	0.06	0.91
Ni	-0.74	0.83	0.89	0.82	-0.51	0.97	0.84	0.88	1.00	0.74	-0.05	0.97
V	-0.58	0.42	0.62	0.55	-0.30	0.62	0.64	0.56	0.74	1.00	-0.12	0.67
Mn	-0.05	-0.10	0.21	0.32	0.60	-0.02	0.03	0.06	-0.05	-0.12	1.00	0.08
Sr	-0.77	0.83	0.95	0.91	-0.36	0.98	0.81	0.91	0.97	0.67	0.08	1.00
Factor 1	0.74	-0.85	-0.94	-0.87	0.44	-0.98	-0.84	-0.93	-0.98	-0.71	-0.03	-0.99
Factor 2	-0.18	-0.24	0.23	0.42	0.84	-0.08	0.01	-0.05	-0.09	-0.07	0.88	0.09
Factor 3	-0.50	-0.45	-0.15	0.00	0.08	-0.11	0.23	-0.31	0.07	0.47	-0.25	-0.00

Table 4: Results of analysis of variance of chemical element concentrations at the site level

Chemical element	SS Effect	df Effect	MS Effect	SS Error	df Error	MS Error	F	p
	Concentration of chemical elements, mg/kg							
Ti	4.1889E+07	5	8.3777E+06	4036990.5	12	336415.9	24.90	0.000006
S	1.2989E+07	5	2.5979E+06	988099.9	12	82341.7	31.55	0.000002
P	2.5711E+04	5	5.1423E+03	2935.2	12	244.6	21.02	0.000015
Mn	1.5638E+05	5	3.1276E+04	31982.7	12	2665.2	11.73	0.000278
Zr	2.1042E+05	5	4.2084E+04	62935.1	12	5244.6	8.02	0.001571
V	2.8112E+04	5	5.6224E+03	4686.1	12	390.5	14.40	0.000103
Sr	1.1378E+05	5	2.2757E+04	1351.1	12	112.6	202.11	0.000000
Zn	3.5551E+05	5	7.1102E+04	142105.0	12	11842.1	6.00	0.005224
Pb	2.8531E+03	5	5.7062E+02	180.3	12	15.0	37.97	0.000001
Y	4.4239E+03	5	8.8479E+02	355.2	12	29.6	29.89	0.000002
Ni	9.6440E+03	5	1.9288E+03	99.5	12	8.3	232.72	0.000000
Cu	6.9765E+03	5	1.3953E+03	64.0	12	5.3	261.78	0.000000
	Concentration coefficient Kc, exceeding background values, times							
Cu*	7.7517E+02	5	1.5503E+02	7.1	12	0.6	261.78	0.000000
Ni*	6.0275E+02	5	1.2055E+02	6.2	12	0.5	232.72	0.000000
Zn*	6.7204E+02	5	1.3441E+02	268.6	12	22.4	6.00	0.005224
Zr*	3.2208E+00	5	6.4416E-01	1.0	12	0.1	8.02	0.001571
Y*	8.0794E+00	5	1.6159E+00	0.6	12	0.1	29.89	0.000002
Ti*	1.9796E+00	5	3.9592E-01	0.2	12	0.0	24.90	0.000006
V*	1.2494E+00	5	2.4988E-01	0.2	12	0.0	14.40	0.000103
Pb*	2.7862E+00	5	5.5724E-01	0.2	12	0.0	37.97	0.000001
S*	9.0204E+00	5	1.8041E+00	0.7	12	0.1	31.55	0.000002
P*	1.7855E-02	5	3.5710E-03	0.0	12	0.0	21.02	0.000015
Mn*	6.9502E-02	5	1.3900E-02	0.0	12	0.0	11.73	0.000278
Sr*	5.4244E-01	5	1.0849E-01	0.0	12	0.0	202.11	0.000000

Table 5: Results of analysis of variance of chemical element concentrations by sampling depth

Chemical element	SS Effect	df Effect	MS Effect	SS Error	df Error	MS Error	F	p
Concentration of chemical elements, mg/kg								
Ti	1489810.6	2	744905.3	4.4436E+07	15	2.9624E+06	0.25145	0.780882
S	138745.6	2	69372.8	1.3839E+07	15	9.2258E+05	0.07519	0.927911
P	1285.5	2	642.7	2.7361E+04	15	1.8241E+03	0.35237	0.708685
Mn	3959.1	2	1979.5	1.8440E+05	15	1.2294E+04	0.16102	0.852725
Zr	10982.7	2	5491.4	2.6237E+05	15	1.7491E+04	0.31395	0.735244
V	22.8	2	11.4	3.2775E+04	15	2.1850E+03	0.00522	0.994791
Sr	308.5	2	154.3	1.1483E+05	15	7.6551E+03	0.02015	0.980078
Zn	18183.8	2	9091.9	4.7943E+05	15	3.1962E+04	0.28446	0.756391
Pb	9.1	2	4.5	3.0243E+03	15	2.0162E+02	0.02248	0.977804
Y	25.6	2	12.8	4.7535E+03	15	3.1690E+02	0.04040	0.960510
Ni	16.9	2	8.5	9.7265E+03	15	6.4844E+02	0.01305	0.987044
Cu	25.0	2	12.5	7.0155E+03	15	4.6770E+02	0.02669	0.973707
Concentration coefficient Kc, exceeding background values, times								
Cu*	2.774	2	1.387	7.7950E+02	15	5.1967E+01	0.02669	0.973707
Ni*	1.058	2	0.529	6.0791E+02	15	4.0527E+01	0.01305	0.987044
Zn*	34.374	2	17.187	9.0630E+02	15	6.0420E+01	0.28446	0.756391
Zr*	0.168	2	0.084	4.0160E+00	15	2.6773E-01	0.31395	0.735244
Y*	0.047	2	0.023	8.6813E+00	15	5.7875E-01	0.04040	0.960510
Ti*	0.070	2	0.035	2.1000E+00	15	1.4000E-01	0.25145	0.780882
V*	0.001	2	0.001	1.4567E+00	15	9.7112E-02	0.00522	0.994791
Pb*	0.009	2	0.004	2.9535E+00	15	1.9690E-01	0.02248	0.977804
S*	0.096	2	0.048	9.6102E+00	15	6.4068E-01	0.07519	0.927911
P*	0.001	2	0.000	1.9001E-02	15	1.2667E-03	0.35237	0.708685
Mn*	0.002	2	0.001	8.1957E-02	15	5.4638E-03	0.16102	0.852725
Sr*	0.001	2	0.001	5.4741E-01	15	3.6494E-02	0.02015	0.980078

of ecological differentiation of sites according to chemical element concentrations (see **Table 4**). All trace elements, without exception, demonstrate high discriminatory ability (significance level $p < 0.05$). With respect to sampling depth, one-way analysis of variance did not identify chemical elements with statistically significant discriminatory ability; for all trace elements, the significance level was $p > 0.05$ (see **Table 5**).

The next stage of this study consisted in constructing a typological scheme of sites within the waste dump impact zone based on trace element concentrations. For this purpose, optimal combinations of concentrations of 12 chemical elements were calculated, allowing the identification of the features of anthropogenic pressure on ecotopes within the waste dump impact zone.

The results of the mathematical modelling can be expressed by the following **Equations 8** and **9**:

$$\begin{aligned} Root_1 = {} & -0.445\times P - 0.026\times S + 0.020\times Ti + \\ & + 2.764\times Y - 0.217\times Zr + 3.105\times Cu + \\ & + 0.006\times Zn + 0.146\times Pb - 1.925\times Ni - \\ & - 0.003\times V + 0.151\times Mn - 0.312\times Sr + 146.768, \end{aligned} \quad (8)$$

$$\begin{aligned} Root_2 = {} & 0.084\times P + 0.025\times S - 0.014\times Ti - \\ & - 0.962\times Y + 0.119\times Zr + 0.139\times Cu + \\ & + 0.031\times Zn - 0.053\times Pb + 1.084\times Ni + \\ & + 0.049\times V - 0.042\times Mn - 0.040\times Sr - 37.736, \end{aligned} \quad (9)$$

Where:

$Root_i$ - are canonical discriminant functions, axes of the typological scheme of edaphotopes within the waste dump impact zone.

The first axis of the typological scheme, $Root_1$ (see **Figure 4**), explains 94.2% of the total variance. The highest values of the canonical discriminant function $Root_1$ are characteristic of the location of site No. 4 (foot of the waste dump), where the edaphotope is formed by drainage sludge. The lowest values of $Root_1$ are observed for the ecotopes of sites No. 6 (pine forest) and No. 1 (natural soil). The values of the first discriminant function $Root_1$ depend on the concentrations of several chemical elements: Sr ($r = 0.96$), Y ($r = 0.96$), Ti ($r = 0.92$), Cu (correlation coefficient $r = 0.91$), Ni ($r = 0.88$), Pb ($r = -0.85$), and Zn ($r = -0.83$). The first axis of the typological scheme, $Root_1$, also reflects an increase in

the level of anthropogenic pressure. A strong relationship between the values of the $Root_1$ function and the soil pollution index *PI* (pollution index) as well as the total pollution index *Zc* for heavy metals is characterized by correlation coefficients of r = 0.89 and r = 0.88, respectively. The less disturbed sites No. 1 and No. 6 are characterized by higher P contents (an indicator of soil fertility). A decrease in anthropogenic pressure is reflected by the following ecological-geochemical gradient: site No. 4 → site No. 2 → sites No. 1, 3, 5, and 6.

The second axis of the typological scheme, $Root_2$ (see **Figure 5**), additionally explains only 3.3% of the total variance. Low values of the canonical discriminant function $Root_2$ are characteristic of the locations of site No. 3 (lake shoreline) and site No. 5 (birch forest). The values of the second discriminant function $Root_2$ depend on the concentration of Zr (correlation coefficient r = -0.85), Mn (r = -0.68), and S (r = 0.56). The two-dimensional typological scheme (see **Figure 5**) explains 97.5% of the total variance caused by differences between ecotopes in terms of trace element contents. Schematically, it can be represented as a triangle, with site No. 2 (*Robinia pseudoacacia* plantation) located in the center and sites No. 4 (foot of the waste dump), No. 3 (lake shoreline), and No. 6 (pine forest) at the vertices. To explain differences in trace element contents among all sites, the Mahalanobis distance (D_M) was calculated – a multidimensional analogue of the Euclidean distance that accounts for correlations between chemical concentrations. As a result of the calculations, it was found that the most distant sites in the hyperspace of geochemical parameters are site No. 4 and site No. 6 (pine forest), with the squared Mahalanobis distance D_M^2= 78,037 units, as well as site No. 4 and site No. 1 (natural soil), with D_M^2 = 71,162 units. The shortest distance relative to site No. 4 is characteristic of site No. 2, with D_M^2 = 31,138 units.

Although univariate statistical analysis provides substantial insight into the geochemical features of edaphotope formation within the waste dump impact zone, it should be considered a preliminary stage of research. In particular, univariate analysis of variance did not reveal differences between edaphotopes depending on sampling depth (see **Table 5**). This task was successfully addressed using multivariate statistical analysis of the entire dataset, namely canonical discriminant analysis.

The results of the mathematical modelling (see **Figure 5**) can be expressed by the following **Equations 10** and **11**:

$$Root_1 = -0.027\times P - 0.010\times S + 0.001\times Ti + \\ + 0.369\times Y - 0.038\times Zr - 0.262\times Cu - \\ - 0.005\times Zn + 0.843\times Pb + 0.126\times Ni - \\ - 0.044\times V - 0.011\times Mn - 0.106\times Sr + 23.523, \quad (10)$$

$$Root_2 = -0.019\times P - 0.008\times S + 0.004\times Ti - \\ - 0.069\times Y - 0.001\times Zr + 0.082\times Cu - \\ - 0.013\times Zn + 0.445\times Pb + 0.285\times Ni - \\ - 0.055\times V - 0.013\times Mn - 0.115\times Sr + 6.059, \quad (11)$$

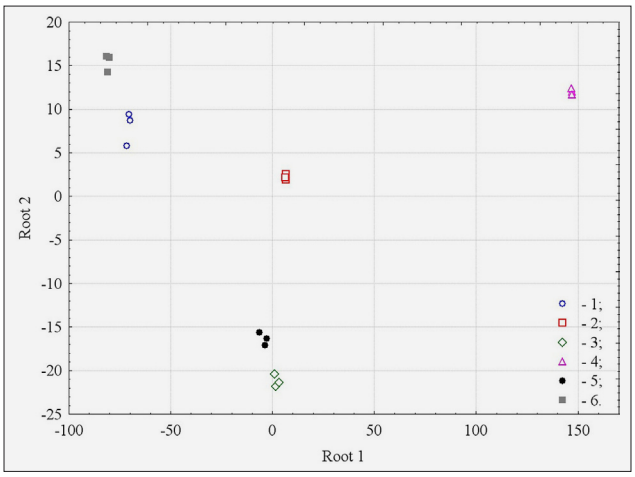


Figure 6: Typological scheme of sites within the waste dump impact zone (site numbering is given in **Table 1**).

Where $Root_i$ are canonical discriminant functions, axes of the typological scheme of edaphotopes based on the vertical distribution of trace elements.

Overall, 83.3% of the samples were correctly classified. Two deviations from the general patterns of vertical distribution of trace elements were recorded at site No. 5 (birch forest), and one deviation was observed at site No. 1 (natural soil). In all cases, the misclassified samples exhibited properties characteristic of deeper soil horizons. Thus, even in surface soil layers, certain features of trace element distribution are present.

The first axis of the typological scheme, $Root_1$ (see **Figure 6**), explains 88.0% of the total variance. The highest values of the canonical discriminant function $Root_1$ are characteristic of sampling locations at a depth of 15 cm. The values of the first discriminant function $Root_1$ depend on the concentrations of the following chemical elements: P (correlation coefficient r = -0.23), Zr (r = -0.21), Ti (r = -0.16), Mn (r = -0.13), and Zn (r = 0.21). Thus, with increasing depth, a tendency toward decreasing concentrations of many trace elements is observed, although the correlation coefficients are characterized by low values. Macroelements were not used for mathematical modelling; however, correlations with the first discriminant function $Root_1$ were also determined for them. For Al, Fe, Mg, Ca, and Si, no differences in vertical distribution were observed, and the correlation coefficients are equal to zero. The second axis of the typological scheme, $Root_2$ (see **Figure 6**), additionally explains 12.0% of the total variance. Low values of the canonical discriminant function $Root_2$ are characteristic of sampling locations at depths of 5 and 15 cm, whereas high values are observed at a depth of 10 cm. The values of the second discriminant function $Root_2$ depend on the concentrations of Mn (correlation coefficient r = -0.85), Ti (r = 0.16), and Zr (r = 0.11). For macroelements, relationships with the concentrations of K (r = 0.28) and Ca (r = -0.30) were observed.

The two-dimensional typological scheme (see **Figure 7**) explains 100.0% of the total variance resulting from

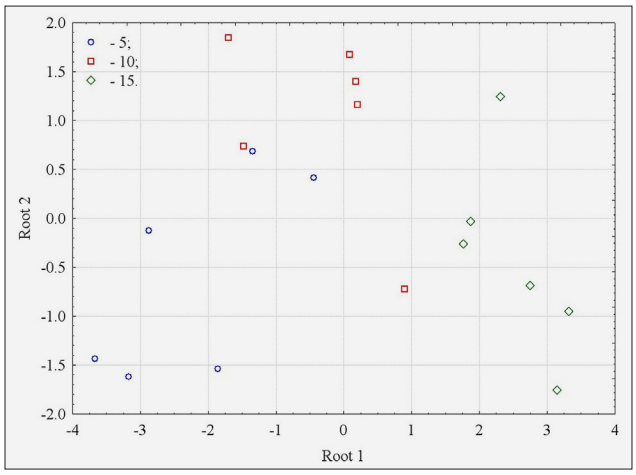


Figure 7: Typological scheme of ecotopes based on the vertical distribution of trace elements (legend: 5, 10, 15 – sampling depth, cm).

differences in trace element contents with depth. Schematically, it can be represented as a triangle.

Sampling locations at a depth of 15 cm are characterized by the highest values of the $Root_1$ function, locations at a depth of 10 cm – by the highest values of the $Root_2$ function, and locations at a depth of 5 cm – by the lowest values of both discriminant functions. As a result of the calculations, it was found that the most distant locations in the hyperspace of geochemical parameters are those at depths of 5 cm and 15 cm, with the squared Mahalanobis distance $D_M^2 = 27.2$ units, as well as those at depths of 10 cm and 15 cm, with $D_M^2 = 12.1$ units. The shortest distance is characteristic of locations at depths of 5 cm and 10 cm, with $D_M^2 = 7.6$ units. Thus, the vertical distribution of trace elements forms an expected geochemical sequence: 5 cm → 10 cm → 15 cm.

4. Conclusions

As a result of the study of the trace element composition of soils within the impact zone of the "Bohdanka" coal mine waste dump belonging to the Lublin Coal Basin, the following conclusions can be drawn:

1. The distribution of trace elements in soils within the waste dump impact zone is characterized by pronounced heterogeneity. Compared with mean values, site No. 4 (foot of the waste dump) exhibits elevated concentrations of 9 out of 12 chemical elements: S, Ti, V, Ni, Cu, Zn, Sr, Y, and Pb, while only P shows a low concentration. At site No. 2, elevated concentrations are characteristic of P, S, Mn, and Pb. Maximum concentrations of Mn and Zr are typical of sites No. 3 and No. 5, whereas maximum P concentrations are observed at site No. 6.
2. The highest exceedances of maximum permissible concentrations (MPC) at the studied sites are characteristic of three chemical elements: Cu (MPC exceedance in the range of 2.5–22.3 times), Ni (2.8–20.1 times), and Zn (0.3–30.0 times).
3. Site No. 4 is characterized by a hazardous level of soil contamination (total pollution index Zc = 53.1–76.5), while site No. 2 is located at the upper limit of the permissible contamination level with a transition to a moderately hazardous category (Zc = 10.8–15.1). The remaining sites are characterized by permissible contamination levels.
4. Based on the absolute contents in the soils of the studied sites, three groups and three subgroups of trace elements can be distinguished:
   I – Ti (mean concentration 4854 mg/kg);
   II – S (mean concentration 804 mg/kg);
   III.1 – P, Mn, Zr (mean concentration 353–590 mg/kg);
   III.2 – V, Sr, Zn (mean concentration 86–145 mg/kg);
   III.3 – Pb, Y, Ni, Cu (mean concentration 21–26 mg/kg).
5. Based on concentration coefficient values, three groups of chemical elements can be identified:
   I. Cu, Ni, Zn (mean concentration coefficients 3.8–6.9 times);
   III. Zr, Y, Ti, V, Pb, S (mean concentration coefficients 0.7–1.4 times);
   III. P, Mn, Sr (mean concentration coefficients 0.2–0.5 times);
6. Multivariate analysis (principal component and discriminant analyses) revealed an ordered structure of ecotopes within the waste dump impact zone and strong associations among trace elements. The main geochemical pattern is characterized by an inverse relationship between phosphorus content (r = 0.74) and the concentrations of Sr, Ni, Cu, Ti, Pb, Y, S, Zn, and V (r = −0.71 to −0.99). The identified environmental gradients reflect combined geogenic conditions and anthropogenic influence, with a strong relationship to soil pollution indices (PI and Zc).
7. Multivariate canonical discriminant analysis revealed features of trace element distribution with depth in the upper soil layers. The vertical distribution forms a geochemical sequence: 5 cm → 10 cm → 15 cm.
8. The developed mathematical models enable refinement of ecological gradients of chemical element distribution in soils, primarily heavy metals, in the upper soil layers.

The study confirms that the distribution of trace elements in soils within the waste dump impact zone is controlled by a combination of geogenic and anthropogenic factors related to mining activities. The enrichment of Cu, Zn, and Ni near the waste dump indicates a significant technogenic impact and active processes of element migration and accumulation. Multivariate statistical analysis revealed key environmental gradients governing the spatial differentiation of chemical elements.

These gradients reflect both depositional conditions and secondary redistribution processes driven by hydrological and physicochemical factors. The findings improve the understanding of trace element migration in technogenically disturbed soils and can be applied for environmental monitoring, ecological risk assessment, and remediation strategies in mining regions.

5. References

Abramowicz, A. K., Rahmonov, O., Fabiańska, M. J., Nádudvari, Á., Chybiorz, R., & Michalak, M. (2021). Changes in soil chemical composition caused by self-heating of a coal-waste dump. *Land Degradation & Development, 32*(15), 4340–4349. https://doi.org/10.1002/ldr.4040

Abramowicz, A., & Rahmonov, O. (2024). Element cycling at thermally active coal-waste dumps: A case study of *Calamagrostis epigejos* and *Solidago canadensis*. *Resources, 13*, 73. https://doi.org/10.3390/resources13060073

Adamenko, Y.S., Arkhypova, L.M., & Mandryk, O.M. (2017). Territorial normative of quality of hydroecosystems of protected territories. *Hydrobiological Journal*, 53(2), 50–58. https://doi.org/10.1615/HydrobJ.v53.i2.50

Bohdan, K., Sracek, O., Mihaljevič, M., Knésl, I., & Majer, V. (2018). Geochemistry and environmental impact of neutral drainage from an uraniferous coal waste heap. *Journal of Geochemical Exploration, 191*, 1–21. https://doi.org/10.1016/j.gexplo.2018.05.001

Bun, R., Marland, G., Oda, T., See, L., Puliafito, E., Nahorski, Z., Jonas, M., Kovalyshyn, V., Ialongo, I., Yashchun, O., & Romanchuk, Z. (2024). Tracking unaccounted greenhouse gas emissions due to the war in Ukraine since 2022. *Science of the Total Environment, 914*, 169879. https://doi.org/10.1016/j.scitotenv.2024.169879

Fatieiev, A.I., Pashchenko, Ya.V. (2003). *Background content of trace elements in soils of Ukraine.* National Science Centre, Kharkiv, 117 p. (In Ukrainian).

Kantardzic, M. (2020). *Data mining. Concepts, models, methods, and algorithms.* 3rd ed., Wiley-IEEE Press, Hoboken, 639 p.

Krzeszowska, E. (2019). Geochemistry of the Lublin Formation from the Lublin Coal Basin: Implications for weathering intensity, palaeoclimate and provenance. *International Journal of Coal Geology*, 216, 103306. https://doi.org/10.1016/j.coal.2019.103306

Krzyszowska Waitkus, A. (2022). Sustainable reclamation practices for a large surface coal mine in shortgrass prairie, semiarid environment (Wyoming, USA): case study. *International Journal of Coal Science & Technology*, 9, 32. https://doi.org/10.1007/s40789-022-00502-3

Kyrylchuk, A.A., Bonishko, O.S. (2011). *Soil chemistry. Fundamentals of theory and practice.* Ivan Franko National University of Lviv, 354 p. (In Ukrainian).

Lewińska-Preis, L., Szram, E., Fabiańska, M. J., et al. (2021). Selected ions and major and trace elements as contaminants in coal-waste dump water from the Lower and Upper Silesian Coal Basins (Poland). *International Journal of Coal Science & Technology, 8*, 790–814. https://doi.org/10.1007/s40789-021-00421-9

Lyashenko, V., Andreev, B. & Dudar, T. (2022). Substantiation of mining-technical and environmental safety of underground mining of complex-structure ore deposits. Mining of Mineral Deposits, 16(1), 43–51. https://doi.org/10.33271/mining16.01.043

Marcisz, M., Probierz, K., & Gawor, Ł. (2020). Possibilities of reclamation and using of large-surface coal mining dumping grounds in Poland. *Gospodarka Surowcami Mineralnymi, 36*(1), 105–122. https://doi.org/10.24425/gsm.2020.132546

Misiak, J. (2012). Quality of coal from exploited seams in LW "Bohdanka" S.A. (Lublin Coal Basin). *Gospodarka Surowcami Mineralnymi – Mineral Resources Management, 28* (4), 137–149. https://doi.org/10.2478/v10269-012-0034-y

Monteiro, M., Santos, P., Marques, J. E., et al. (2024). Assessment of mobile mercury concentration in soils of an abandoned coalfield waste pile in Douro region: The Fojo waste pile (Portugal) study case. *Journal of Soils and Sediments, 24*, 2068–2077. https://doi.org/10.1007/s11368-024-03786-x

Nádudvari, A., Kozielska, B., Abramowicz, A., Fabiańska, M., Ciesielczuk, J., Cabała, J., & Krzykawski, T. (2021). Heavy metal- and organic-matter pollution due to self-heating coal-waste dumps in the Upper Silesian Coal Basin (Poland). *Journal of Hazardous Materials, 412*, 125 244. https://doi.org/10.1016/j.jhazmat.2021.125244

Nersesyan, A., Mišík, M., Cherkas, A., Serhiyenko, V., Staudinger, M., Holota, S., Yatskevych, O., Melnyk, S., Holzmann, K., Knasmüller, S. (2021). Use of micronucleus experiments for the detection of human cancer risks: a brief overview. *Proceedings of the Shevchenko Scientific Society. Medical Sciences*, 65(2). https://doi.org/10.25040/ntsh2021.02.05

Nieć, M., Sermet, E., & Salamon, E. (2023). Variation of coal quantity accumulated in the Mississippian to Pennsylvanian coal seams (Upper Silesia and Lublin Coal basins, Poland). *Geological Quarterly, 67*, 8. https://doi.org/10.7306/gq.1678

Oleńska, E., Małek, W., Wójcik, M., et al. (2023). Bacteria associated with Zn-hyperaccumulators *Arabidopsis halleri* and *Arabidopsis arenosa* from Zn–Pb–Cd waste heaps in Poland as promising tools for bioremediation. *Scientific Reports, 13*, 12606. https://doi.org/10.1038/s41598-023-39852-6

Popovych, V. V., & Voloshchyshyn, A. I. (2019). Environmental impact of devastated landscapes of Volhynian Upland and Male Polisya (Ukraine). *Environmental Research, Engineering and Management, 75*(3), 33–45. https://doi.org/10.5755/j01.erem.75.3.23323

Popovych, V., Bosak, P., Petlovanyi, M., Telak, O., Karabyn, V., & Pinder, V. (2021). Environmental safety of phytogenic fields formation on coal mines tailings. *News of the National Academy of Sciences of the Republic of Kazakhstan, Series of Geology and Technical Sciences, 2*(446), 129–136. https://doi.org/10.32014/2021.2518-170X.44

Popovych, V. V., Skrobala, V., Kopylov, V., & Kopystynskyi, Y. (2025). Heavy metals distribution in water and soil of the coastal zone of the Styr River (Ukraine) and its tributaries. *Journal of Ecological Engineering, 26*(2), 1–14. https://doi.org/10.12911/22998993/196042

Pukish, A., Mandryk, O., Arkhypova, L., Syrovets, S., & Hryniuk, D. (2024). Mathematical modeling of pollution of underground aquifers due to mining of minerals. *Mining of Mineral Deposits, 18*(3), 94–103. https://doi.org/10.33271/mining18.03.094

Pukish, A.V., Sydorenko, O.I., Mandryk, O.M., Korobeinykova, Y.S., Tuts, O.M. (2023). The effect of pollutants on the content of nutrients in soil. *Nafta-Gaz*, 79(4), 266–277. https://doi.org/10.18668/NG.2023.04.06

Salgado, L., Aparicio, L., Afif, E., et al. (2024). A second life for mining waste as an amendment for soil remediation. *Journal of Material Cycles and Waste Management, 26*, 2971–2979. https://doi.org/10.1007/s10163-024-02013-6

Serhiyenko, V., Serhiyenko, A. (2019). Diabetic cardiac autonomic neuropathy. In: *The Diabetes Textbook: Clinical Principles, Patient Management and Public Health Issues*, 825–850. https://doi.org/10.1007/978-3-030-11815-0_53

Serhiyenko, V. V., & Serhiyenko, A. A. (2022). Diabetes mellitus and congestive heart failure. *Mizhnarodnij Endokrinologichnij Zhurnal, 18*(1), 57–69. https://doi.org/10.22141/2224-0721.18.1.2022.1146

Shmatkov, H. H., & Yakovyshyna, T. F. (2018). System of indicators for comprehensive assessment of multi-element heavy metal pollution of soils in urban ecosystems. *Ecological Sciences, 1*(20), 25–29. (In Ukrainian).

Skrobala, V., Popovych, V., & Pinder, V. (2020). Ecological patterns for vegetation cover formation in the mining waste dumps of the Lviv-Volyn coal basin. *Mining of Mineral Deposits, 14*(2), 119–127. https://doi.org/10.33271/mining14.02.119

Skrobala, V.M., Popovych, V.V., Bosak, P.V., Shuplat, T.I. (2022a). Prediction of changes in the vegetation cover of Ukraine due to climate warming. *Naukovyi Visnyk Natsionalnoho Hirnychoho Universytetu, 4*, 96–105. https://doi.org/10.33271/nvngu/2022-4/096

Skrobala, V., Popovych, V., Tyndyk, O., Voloshchyshyn, A. (2022b). Chemical pollution peculiarities of the Nadiya mine rock dumps in the Chervonohrad Mining District, Ukraine. *Mining of Mineral Deposits, 16*(4), 71–79. https://doi.org/10.33271/mining16.04.071

Tatsiy, R.M., Pazen, O.Yu., Vovk, S.Ya., Ropyak, L.Ya., Pryhorovska, T.O. (2019). Numerical study on heat transfer in multilayered structures of main geometric forms made of different materials. *Journal of the Serbian Society for Computational Mechanics*, 13(2), 36–55. https://doi.org/10.24874/jsscm.2019.13.02.04

SAŽETAK

Raspodjela elemenata u tragovima u tlima zone utjecaja ugljenokopa Bogdanka (Lublinski ugljeni bazen): geokemijska perspektiva

U ovome radu prikazani su rezultati istraživanja sadržaja kemijskih elemenata u tlima unutar zone utjecaja odlagališta rudničkoga otpada, s posebnim naglaskom na rudnik ugljena Bogdanka (Lublinski ugljeni bazen) i njegov utjecaj na okolne ekosustave. Geokemijska analiza temelji se na podatcima o koncentracijama 12 kemijskih elemenata (P, S, Ti, Y, Zr, Cu, Zn, Pb, Ni, V, Mn, Sr) u tlima na šest lokacija pogođenih odlagalištem otpada. Matematičko modeliranje provedeno je uspostavljanjem funkcionalnih odnosa između koncentracija kemijskih elemenata. Na temelju apsolutnih koncentracija u tlima istraživanih područja izdvojene su sljedeće skupine mikroelemenata: I – Ti (4854 mg/kg); II – S (804 mg/kg); III.1 – P, Mn, Zr (353 – 590 mg/kg); III.2 – V, Sr, Zn (86 – 145 mg/kg); III.3 – Pb, Y, Ni, Cu (21 – 26 mg/kg). Lokalitet br. 4 (podnožje jalovišta) obilježen je visokim stupnjem onečišćenja tla (ukupni indeks onečišćenja Zc = 53,1 – 76,5), dok se lokalitet br. 2 nalazi na gornjoj granici dopuštene razine onečišćenja s prijelazom u umjereno opterećenu zonu (Zc = 10,8 – 15,1). Ostali lokaliteti karakterizirani su dopuštenim razinama onečišćenja. Diskriminantnom analizom utvrđena je raspodjela mikroelemenata po dubini u površinskim slojevima tla, pri čemu je definiran geokemijski slijed 5 cm, 10 cm i 15 cm. Razvijeni matematički modeli omogućuju kvantifikaciju ekoloških gradijenata raspodjele kemijskih elemenata u tlima, osobito teških metala, u gornjim slojevima tla.

Ključne riječi:
ugljenokop, jalovište, elementi u tragovima, geokemijski procesi, sigurnost okoliša, tehnološka sigurnost, ljudsko zdravlje

Author's contribution

Vasyl Popovych (Dr. Sci., Professor) proposed and defined the idea of the scientific article, managed the field research, provided suggestions for interpretation of the results and graphical presentation of the data, adjustment of the article. **Viktor Skrobala** (PhD, Associate Professor)**, Victoria Serhiyenko** (Dr. Sci. in Medicine, Professor)**, Taras Boyko** (PhD)**, Yevhen Kobko** (Dr. Sci. in Law, Professor)**, Oksana Telak** (Dr. hab.)**, Ostap Kit** (PhD student) **and Iryna Fediv** (PhD) performed the field work, provided funding for the fieldwork, data collection and modelling, participation in the field research and analysis, graphically presented the data, and gave input into the discussion and conclusion sections. All authors have read and agreed to the published version of the manuscript.